Journal of Metals, Materials and Minerals, Vol.27 No.1 pp.13-23, 2017

Mechanical and Thermal Properties of Eucalyptus Fiber Composites from Blend between Biodegradable Poly(Butylene Succinate) and Recycled PET

Nattakarn HONGSRIPHAN *, Phoorinat DANGMANEE, Mookyada MANKRUT
and Warunkarn JANTARAKA

Department of Materials Science and Engineering, Faculty of Engineering and Industrial Technology, Silpakorn University, Nakhon Pathom, Thailand

Abstract

This study was to enhance rigidity and to reduce cost of the Poly(Butylene Succinate) **(**PBS)-based composites by blending with recycled poly(ethylene terephthalate) (r-PET) and Eucalyptus fibers. Prior compounding, Eucalyptus fibers were treated with alkali and γ-methacryloxypropyl trimethoxysilane (MPS) solution. PBS and r-PET were melt blended in a twin-screw extruder with the weight ratio of 95/5, 90/10, and 80/20 wt%, and compounded with MPS treated Eucalyptus fibers using fiber loading of 3, 5, and 7 wt% of composites. It was found that r-PET increased rigidity of PBS matrix but reduced impact resistance. Glass transition temperature of PBS and r-PET shifted toward each other indicating compatibility between them via transesterification. Chemical shifts in NMR indicated chemical interaction between PBS matrix and MPS grafted on Eucalyptus fibers. Blending PBS with r-PET and Eucalyptus fibers synergistically increased rigidity for the PBS matrix. Composites of PBS/r-PET 80/20 wt% blends with 7 wt% fiber presented Young's modulus 67.3% higher than that of neat PBS. The impact property depended on r-PET content. The composites from PBS/r-PET 95/5 wt% blend was the best. SEM images revealed the fine particles of r-PET domains dispersed inside PBS matrix, and wetting of PBS on silane treated fibers was clearly obtained.

Keywords: Short fiber composite; Poly(butylene succinate); Recycled PET; Eucalyptus fibers; MPS silane

Introduction

Poly(butylene succinate) (PBS) is an aliphatic polyester that has been increasing commercial interest due to its ability to be 100% biobase with lower cost in the near future. Currently, PBS is a petroleum-based biodegradable polymer that can be synthesized by poly condensation of succinic acid with 1,4-butanediol.(1) With continuing development of PBS with higher molecular weight or copolymerization route, it is expected to be applied in the engineering field, such as consumer goods, electrics and electronics. Nowadays, the main drawback for using PBS in commercial application is high cost. Therefore, there have been development of PBS in composite form in order to improve mechanical properties and this would provide a cost reduction solution. There have been researchers attempting to produce composites of PBS by reinforcing with lignocellulosic fillers such as jute (2), sisal (3), coconut, sugarcane, bagasse, curaua(4), or inorganic fillers such as calcium carbonate nanoparticle(5) and carbon nanotubes (6). Although tensile modulus or flexural modulus of the PBS-based composites were enhanced with these reinforcement, the advantage of PBS being flexible polymer like low-density polyethylene (LDPE) was deteriorated.

Poly(ethylene terephthalate) (PET) is one of the most important and extensively used plastics in the world, especially for manufacturing beverage containers. Most PET bottles used as beverage containers are thrown away after single usage and disposed PET bottles are managed by landfill and incineration, which are causing serious environmental problems. One possible solution is blending recycled PET with other polymers since recycled PET could offer rigidity or introduce toughness into the blends. Our previous research (7) improved mechanical properties of PBS by melt blending with recycled PET flakes from drinking bottles. Contents of r-PET blended were 1, 2, and 5% by weight. It was found that PBS/r-PET blends had higher tensile modulus but reduced flexibility

---

* Corresponding author. E-mail: Hongsriphan_N@su.ac.th

DOI: 10.14456/jmmm.2017.2

with higher PET content. For DSC analysis, it was found that blending PBS with r-PET increased crystallinity of PBS matrix due to nucleating effect of r-PET dispersed spheres. However, melt blending between them required high temperature enough to melt r-PET flakes, so it caused thermal scission in PBS molecules as evidenced in TGA analysis.

In this work, post-consumer recycled PET (r-PET) from drinking water bottles was grinded and melt blended into PBS with the weight ratio of 95/5, 90/10, 85/15 and 80/20 wt%. Then, the blends were compounded with treated Eucalyptus fibers with the goal to enhance stiffness of the PBS-based composites using fiber reinforcement. Eucalyptus fibers was treated with alkali and γ-methacryloxy propyl trimethoxysilane (MPS) for better compatibility with PBS/r-PET blends. Tensile and impact properties of the blends and their composites were evaluated. Morphological and thermal properties of the blends and their composites were characterized in order to evaluate how mechanical enhancement was obtained. Moreover, ^{1}H-NMR spectroscopies was carried out to analyze chemical interaction between polymer matrix and reinforced fibers.

Materials and Experimental Procedures

Materials

Poly(butylene succinate) (PBS) pellets (GS Pla®, Grade FZ91PD) with MFI of 6 g/10 min (190°C, 2.16 kg) was purchased from Mitsubishi Chemicals, Japan. Recycled poly(ethylene terephthalate) (r-PET) flakes were obtained from mechanical grinding post-consumer PET drinking water bottles. These bottles under the same brand name were collected, cleaned with tap water and detergents, and then air dried prior grinding. R-PET were grinded to have flake size less than 10 mm. Eucalyptus fibers were kindly supplied by SCG Paper Co Ltd, Thailand. These fibers were alkali treated with 10 wt% Sodium hydroxide for using in craft paper, which they were used as received for further silane treatment. γ-metharyloxypropyl trimethoxysilane (MPS) was purchased from Sigma- Aldrich Co., LLC. Ethanol and Acetic acid were purchased from Union Intraco and ACI Labscan, Thailand, respectively.

Silane treatment of Eucalyptus fibers

Alkali Eucalyptus fibers were silane treated with γ-methacryloxypropyltri methoxy silane (MPS). Silane solution was prepared in water-ethanol solution (40:60 wt/wt) using MPS concentration of 3 wt% fiber weight and liquid/fiber ratio of 40:1. The solution pH was adjusted to 4 using diluted acetic acid and stirred continuously for 1 h. Alkali treated Eucalyptus fibers (oven dried) were soaked in silane solution for 3 h, filtered and rinsed thoroughly with distilled water several times, and dried in an air-circulating oven at 70°C for 48 h.

Sample preparation for PBS/r-PET blends and silane treated Eucalyptus fiber composites

Before blending, PBS pellets and r-PET flakes were pre-dried at 60 and 120°C for 6 h in an air-circulating oven to remove moisture. Dried PBS pellets and r-PET flakes were melt compounded in the weight ratio of 100/0, 95/5, 90/10, 85/15, and 80/20 wt% using a co-rotating twin-screw extruder (SHJ-25, L/D 40, Yongteng, China). The temperature profile of the extruder/die were set up 130-150-200-260-260-200-150-130°C, to provide melt blending of the polymer blend. The screw speed was set at 60 rpm. The extrudeate was water cooled, pelletized, and dried right after the palletization.

For composites, the blends with 5, 10 and 20 wt% of r-PET were compounded with MPS treated Eucalyptus fibers, which fibers were varied 3, 5 and 7 wt% of the composites. The compounding was carried under the same temperature profile of the PBS/r-PET blending. Compositions of the blends and their composites were summarized in Table 1. Dogbone and impact specimens were fabricated by injection moulding (Battenfeld BA 250 CDC, Austria) using the temperature profile of 200 to 230°C from feed zone to nozzle and the mold temperature of 50°C.

.

Table 1 Compositions of PBS/r-PET blends and Silane treated Eucalyptus fiber composites.

Sample code	PBS (wt%)	r-PET (wt%)	Silane treated Eucalyptus fibers (wt%)
Neat PBS	100.00	0.00	0
PBS/r-PET 95/5	95.00	5.00	0
PBS/r-PET 90/10	90.00	10.00	0
PBS/r-PET 80/20	80.00	20.00	0
PBS95/r-PET5/Euca3	92.15	4.85	3
PBS95/r-PET5/Euca5	90.25	4.75	5
PBS95/PET5/Euca7	88.35	4.65	7
PBS90/r-PET10/Euca3	87.30	9.70	3
PBS90/r-PET10/Euca5	85.50	9.50	5
PBS90/r-PET10/Euca7	83.70	9.30	7
PBS80/r-PET20/Euca3	77.60	19.40	3
PBS80/r-PET20/Euca5	76.00	19.00	5
PBS80/r-PET20/Euca7	74.40	18.60	7

Characterization and testing

Alkali treated and MPS treated Eucalyptus fibers were characterized by a Fourier transmittance Infrared (FT-IR) spectrometer (Vertex 70, Bruker, USA), which the spectra were recorded between 4,000 and 400 cm^{-1}. Samples were placed on the ATR attachment and a minimum of 32 scans were averaged with a resolution of 2 cm^{-1} within 4,000–400 cm^{-1} range.

Tensile test was performed in accordance to ASTM-D638 using a Universal Testing Machine (Instron, Model 5969, Instron Engineering Corporation, USA). The IV-type specimens of neat PBS, PBS/r-PET blends and Eucalyptus fiber reinforced composites were conditioned at 25°C for 48 h prior to testing. The testing was performed with a crosshead speed of 10 mm/min. The average and standard deviations of ten measurements was calculated and reported. Data was also analyzed by the One-way analysis of variance (ANOVA) using MINITAB 17.0 software package. Difference among composition change was considered to be statistically significant if $p < 0.05$.

Notched Izod impact test was performed in accordance to ASTM-D256 using an impact tester (Zwick, B5102.202, Germany) with a pendulum hammer of 4.0 J. The test specimens of neat PBS, PBS/r-PET blends and Eucalyptus fiber reinforced composites were conditioned at 25°C for 48 h prior to testing, and then notched. The testing was performed, which the average and standard deviations of ten measurements was calculated and reported. Data was also analyzed by the One-way analysis of variance (ANOVA) using MINITAB 17.0 software package. Difference among composition change was considered to be statistically significant if $p < 0.05$.

Morphology of neat PBS, PBS/r-PET blends and Eucalyptus fiber reinforced composites were examined by a Scanning Electron Microscope (SEM) (Tabletop Microscope TM3030, Hitachi, Japan). Impact fractured specimen surface was platinum coated prior to inspection to avoid electrostatic charging.

FTIR spectra of Eucalyptus fiber reinforced composites were recorded between 4,000 and 400 cm^{-1} with a FT-IR spectrometer, (Vertex 70, Bruker, USA). Samples were placed on the ATR attachment and a minimum of 32 scans were averaged with a resolution of 2 cm^{-1} within the 4,000–400 cm^{-1} range.

The structures of neat PBS and Eucalyptus fiber reinforced composites were determined by a ^{1}H-NMR spectrometer (300-MHz Bruker AC 250, Bruker, USA) at 25°C. Samples were dissolved by Chloroform-d ($CDCl_3$) with a concentration of 3 wt% and filtered for NMR analysis, which tetra-methylsilane (TMF) was used as the internal reference.

Thermal properties of neat PBS, PBS/r-PET blends and Eucalyptus fiber reinforced composite samples were determined under Nitrogen atmosphere using a differential scanning calorimeter (DSC1 Mettler-Toledo, Switzerland). The sample weight used was approximately 5-10 mg weight. The samples were tested in a heat-cool-reheat mode, with the heating rate and the cooling rate of 10°C/min. Temperature scan was performed from -50°C to 270°C. The percentage crystallinity (X_c) was calculated as the following equation:

$$\%X_c = \frac{\Delta H_m}{\Delta H_f^o} \times \frac{100}{w} \qquad (1)$$

where ΔH_m was melting enthalpy of crystalline (J/g), ΔH_f was melting enthalpy of 100% crystalline of PBS (110.3 J/g)$^{(8)}$ or of PET (140.1 J/g)$^{(9)}$, and w was weight fraction of PBS in composites

Results and Discussion

Characterization of MPS treatment on Eucalyptus wood fibers by FTIR

FTIR spectra of alkali treated and MPS treated Eucalyptus fibers are presented in Figure 1. It was found that there was strong and broad absorption peak in the 3,700-3,000 cm^{-1} which attributed to the –OH stretching from the presence of hydroxyl groups (cellulose) in Eucalyptus fibers. Since these received fibers were treated with 10 wt% NaOH, the alkali treatment process effectively removed hemicellulose. This resulted disappearance of the absorption peak at 1,740 cm^{-1} attributed to C=O stretching vibration of hemicellulose.$^{(10)}$ Also, there was absence of characteristic absorption at 1,241 cm^{-1} which corresponded to the C-O-C stretching vibration of the ether group in lignin, indicating that lignin was also removed. Since these fibers were mainly cellulose, the observed strong absorption peak at 1,636-1,638 cm^{-1} was due to adsorbed water that forms hydrogen bonding with hydroxyl groups.$^{(11)}$ The presence of peak at 1,120 cm^{-1} in MPS treated Eucalyptus fibers attributed to Si-O-C bonds, indicating the occurrence of condensation reaction between hydrolysed silane and celluloses in treated Eucalyptus fibers. The small broad peak at 1,030 cm^{-1} and at 893 cm^{-1} implied the existence of poly siloxane network. Moreover, the absorption at 1,431 cm^{-1} for the MPS treated Eucalyptus fibers attributed to O-H bending of carboxylic acids (-COOH)$^{(12)}$. This resulted from multilayer formation occurring between MPS molecules through C=O and O-H groups.

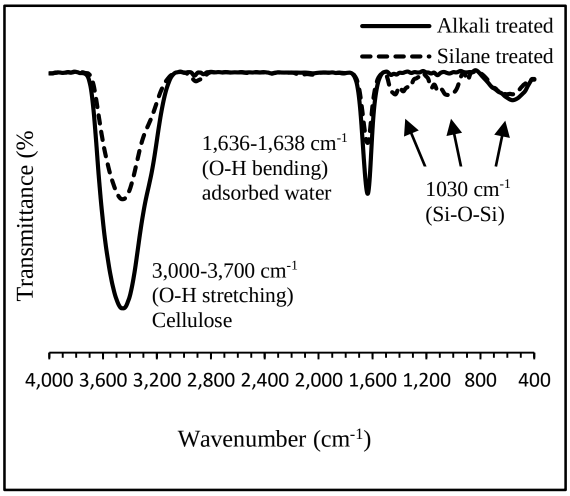

Figure 1. FTIR spectra of alkali treated and MPS treated Eucalyptus fibers.

Tensile properties of PBS/r-PET blends and MPS treated Eucalyptus fiber reinforced composites

In order to study influence of r-PET on rigidity improvement of PBS matrix, the PBS/r-PET blends were compounded and fabricated under the same processing condition for wood fiber reinforced composites. Figure 2 presents Young's modulus, tensile strength and elongation at break of neat PBS and PBS/r-PET blends using r-PET content of 5, 10, and 20 wt%. As expected, PBS/r-PET blends showed higher Young's modulus compared to neat PBS. The Young's moduli of PBS were increased from 296 MPa to 340, 349, and 413 MPa for blending r-PET content of 5, 10, and 20 wt%, respectively. Since PBS and PET were both polyesters, partial miscibility could take place due to transesterification $^{(13)}$ as seen later in DSC results. The compatibility between polymeric phases improved load transfer in the polymer blend from the applied stress..

Tensile strength of the blends were 40.59, 39.73, 40.43 and 39.13 MPa for blending r-PET content of 0, 5, 10 and 20 wt%, respectively. Statistically, these variations were not significantly different except for PBS/r-PET 80/20 wt% blend. Nevertheless, blending PBS with r-PET reduced elongation at break especially for blending r-PET of 20 wt%. It was believed that drawback on toughness resulted from the presence of fine r-PET dispersed phases embedded in PBS matrix which was evident in SEM images. These small particles became stress concentrators for the blends to be broken in brittle behavior.

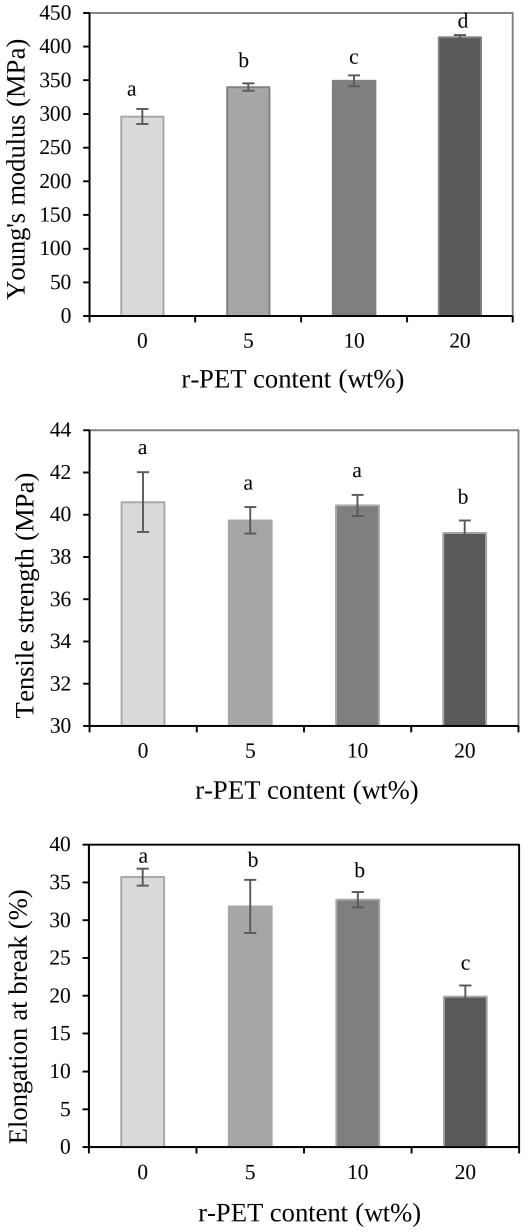

Figure 2. Young's modulus, tensile strength, and elongation at break of neat PBS and PBS/r-PET blends with 5, 10, and 20 wt% r-PET content. Means with the same letter are not significantly different from each other (P>0.05 ANOVA followed by Tukey Method).

Figure 3 presents Young's modulus of composites between PBS/r-PET blends and MPS treated Eucalyptus wood fibers using various composite compositions. In the figure, a dashed line indicated Young's modulus (296 MPa) of neat PBS specimens in this study. Table 2 summarizes Young's modulus of MPS treated Eucalyptus wood fibers reinforced composites, and the modulus increasing in percentage compared to neat PBS. It was seen that these fiber reinforced composites had higher Young's modulus when incorporating higher r-PET content or higher fiber loading. Because of silane treatment, good load transfer between fibers and polymer matrix was expected to occur from proper fiber wetting. For r-PET content of 10 wt% of the blends, they showed synergistic with fiber reinforcement to gain significant increase of Young's modulus in the composites. Anyhow, Young's modulus of PBS/r-PET 80/20 wt% composites was increased linearly with fiber loading.

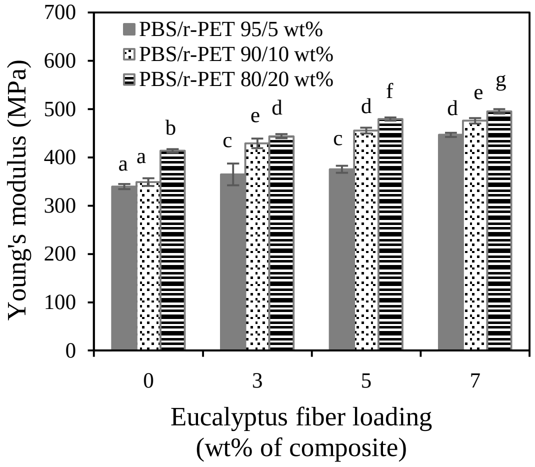

Figure 3. Young's modulus of MPS treated Eucalyptus fiber reinforced PBS/r-PET composites. Means with the same letter are not significantly different from each other (P>0.05 ANOVA followed by Tukey Method).

Table 2 Young's modulus of MPS treated Eucalyptus fiber reinforced composites and modulus increasing percentage.

Blends/Composites	Young's modulus (MPa) (Modulus increasing in % compared to neat PBS)		
	PBS95/r-PET5	PBS90/r-PET10	PBS80/r-PET20
No fibers	339.76 (14.8%)	349.15 (18.0%)	413.59 (39.7%)
3 wt% fibers	364.75 (23.2%)	429.21 (45.0%)	443.88 (50.0%)
5 wt% fibers	375.15 (26.7%)	455.53 (53.9%)	479.42 (62.0%)
7 wt% fibers	446.69 (50.9%)	475.84 (60.8%)	495.33 (67.3%)

Figure 4 shows tensile strength and elongation at break of MPS treated Eucalyptus wood fibers reinforced PBS/r-PET composites. It was found that tensile strength of composites were in the same range despite of different r-PET content or fiber loading.

This was in agreement with these composites using the same silane concentration for fiber treatment. However, elongation at break was reduced with respect to fiber loading even though the blends had different r-PET contents. This indicated that the failure was initiated in the similar fashion that happened at the interfaces between fibers and polymer matrix.

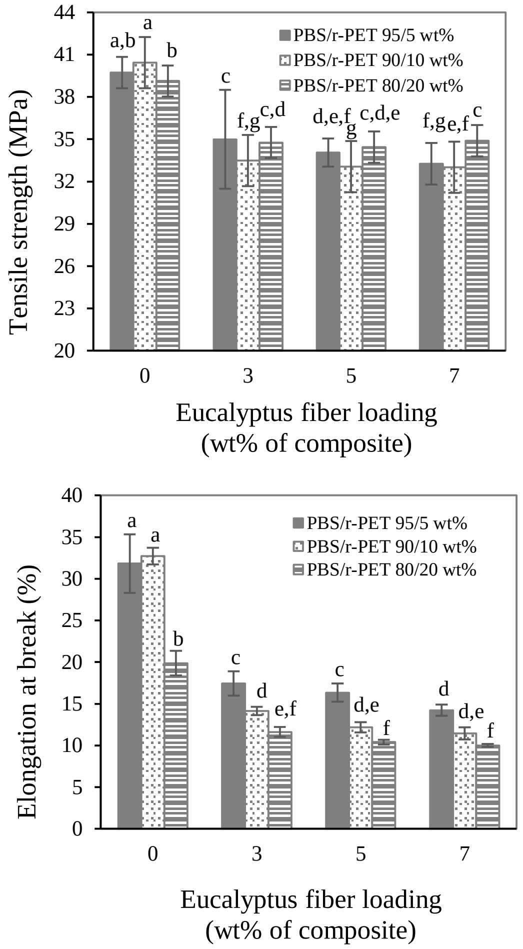

Figure 4. Tensile strength and elongation at break of MPS treated Eucalyptus fiber reinforced PBS/r-PET composites. Means with the same letter are not significantly different from each other (P>0.05 ANOVA followed by Tukey Method).

Impact strength of PBS/r-PET blends and MPS treated Eucalyptus fiber reinforced composites

Figure 5 presented notched Izod impact strength of MPS treated Eucalyptus fiber reinforced PBS/r-PET composites, which impact strength of neat PBS was 9.10 x 10^3 J/m^2. Although blending r-PET enhanced rigidity of PBS, toughness of the PBS matrix was reduced by embedding of rigid r-PET phases that generated sites for crack initiation and propagation. Specimen failure changed from ductility to brittleness with the presence of fine r-PET dispersed phases.

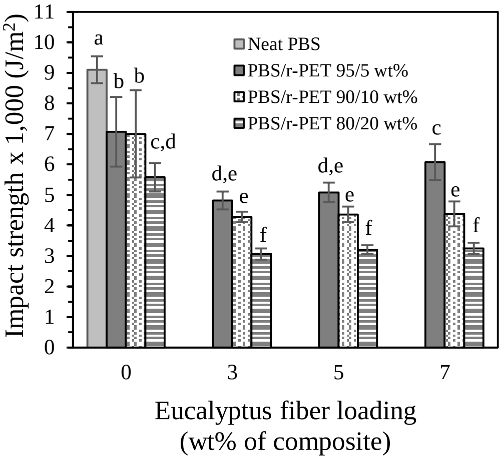

Figure 5. Notched Izod impact strength of MPS treated Eucalyptuswood fibers reinforced PBS/r-PET composites. Means with the same letter are not significantly different from each other (P>0.05 ANOVA followed by Tukey Method).

This was in agreement with the work by A.Pawlak *et al.*(14) which reported that the HDPE/r-PET blends without a compatibilizer showed lower impact strength than the neat polymers.

Reinforcing the blends with fibers further reduced impact strength due to less mobility of PBS molecules by surrounding fibers. Interestingly, only the blends with r-PET of 5 wt% showed increasing of impact strength when reinforcing with MPS treated Eucalyptus fibers in this study. We proposed that these rigid r-PET domains with interfacial adhesion onto PBS matrix acted as shock absorbance before small cracks occurred. Unfortunately, these domains became stress concentrators when there were too many of them embedded in flexible PBS matrix causing rapid crack propagation inside the matrix.

Morphology of PBS/r-PET blends and Eucalyptus fiber reinforced composites

Figure 6 presents SEM of impact fractured surfaces of neat PBS and PBS/r-PET blends in the weight ratio of 95/5, 90/10, and 80/20 wt%, respectively. Under 50X magnification, SEM images showed that the impact fracture surfaces of PBS/r-PET 95/5 wt% was clean and smooth with a few local whitening zones. For PBS/r-PET 90/10 and 80/20 wt% blends, cracking lines were observed indicating crack propagation of brittle behaviour. Under 4,000X magnification, finely PET dispersed phases clearly presented confirming phase separation between hydrophobic PBS matrix and relatively hydrophilic r-PET domains. By using the compounding condition in this study, the dispersed phases of r-PET was less than one micron which provided good reinforcing effect for rigidity enhancement. Unlike PET/PP blend(15), the r-PET dispersed phases did not debond from the PBS matrix leaving no holes in the PBS matrix. This implied that there was good interfacial adhesion between them achieved from transesterification. However, these fine partial-miscible phases became stress propagation sites during high speed loading resulting in decreasing impact resistance of PBS matrix when melt blending with r-PET of 20 wt%.

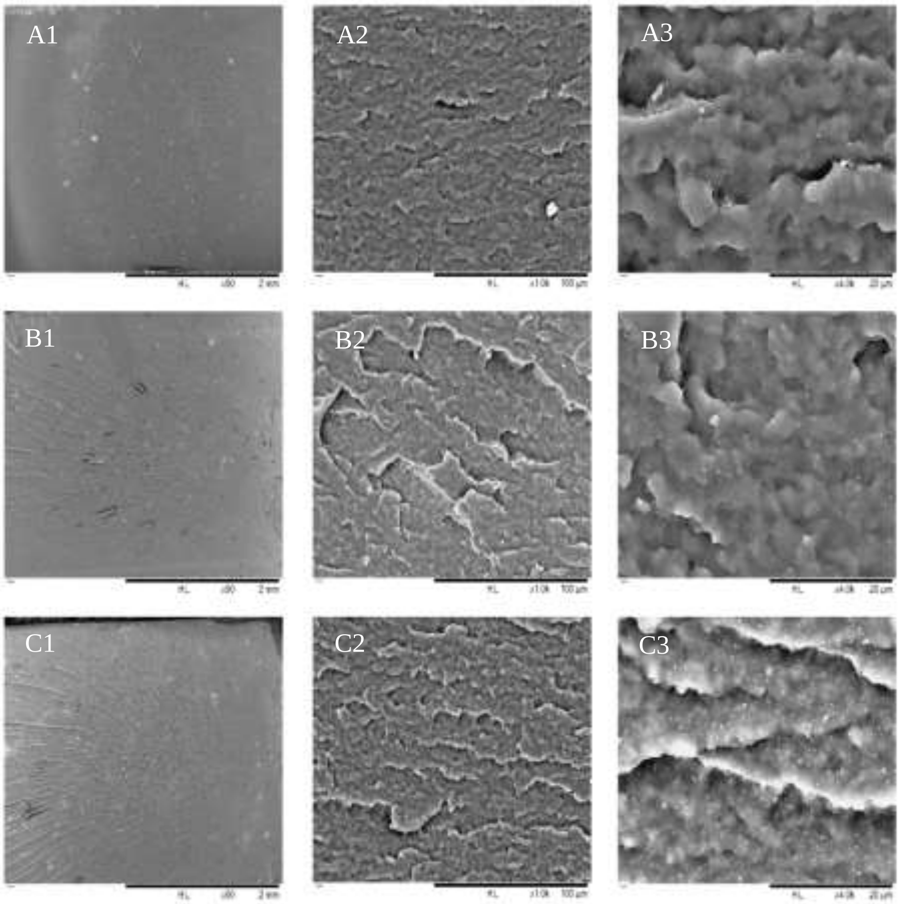

Figure 6 Impact fracture SEM images of PBS/r-PET blends with r-PET content of 5 wt% (A1-3), 10 wt% (B1-3), and 15 wt% (C1-3).

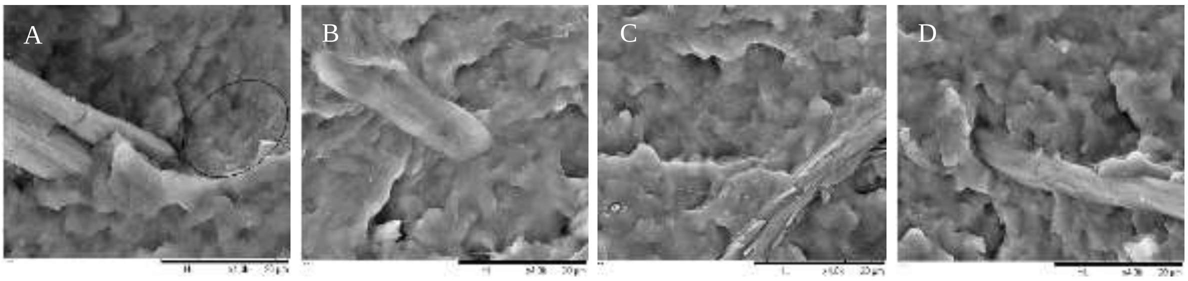

Figure 7 SEM images of impact fracture specimens revealing interfacial adhesion between MPS treated Eucalyptus fibers and PBS matrix; (A) PBS95/r-PET5/Euca3, (B) PBS95/r-PET5/Euca5, (C) PBS80/r-PET20/Euca3, and (D) PBS80/r-PET20/ Euca5.

Figure 7 presents SEM images of impact fracture specimens of Eucalyptus fiber reinforced PBS/r-PET composites. From the images, it is seen that Eucalyptus fibers were wetted by PBS matrix which there was no voids observed around the fibers. There were fine PET dispersed domains embedded in the PBS matrix, at which there were small pits indicating that these fine PET domains were peeled out of the PBS matrix during the shock loading.

Characterization of MPS treated Eucalyptus fiber reinforced composites by ^{1}H-NMR

In order to study chemical interaction between phases, the ^{1}H-NMR studies of neat PBS and PBS95/r-PET5/Euca5 composites were carried out for comparison. Figure 8(a) presents the ^{1}H-NMR spectrum of neat PBS which the chemical shifts d = 4.119, 1.689 and 2.626 ppm represented the H_1, H_2 and H_3, respectively.(16) Figure 8(b) presents the ^{1}H-NMR spectrum of PBS95/r- PET5/Euca5 composites, which the similar spectrum was obtained except that there was the proton, H_1^* representing the proton of bonded carbon in the MPS after MPS was grafted to PBS.(17) Therefore, the simplified illustration of MPS molecules grafting on Eucalyptus wood fibers and PBS molecules could be proposed as shown in Figure 9. These interactions between PBS matrix and silane grafted fibers provided good load transfer between phases resulting in stiffness improvement these fiber reinforced composites.

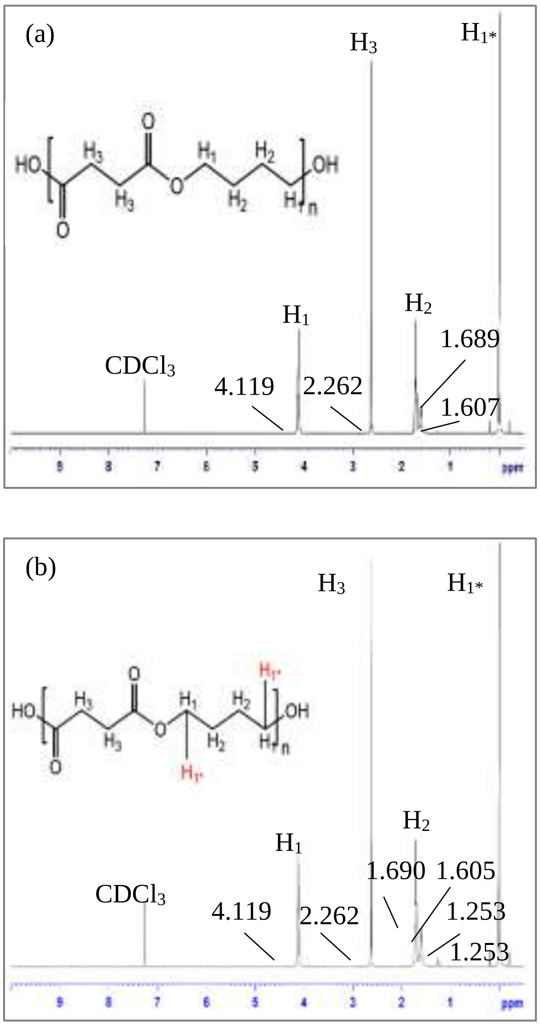

Figure 8. ^{1}H-NMR spectra of (a) neat PBS and (b) PBS95/r-PET5/Euca7 composites.

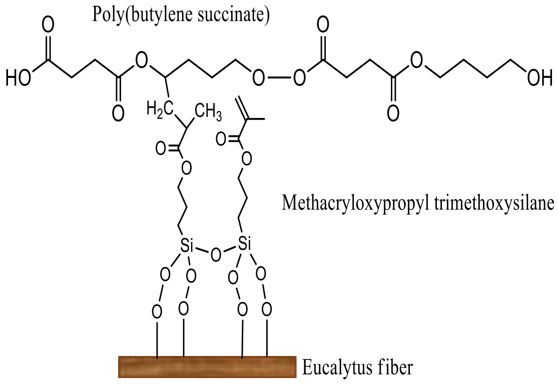

Figure 9. Simplified illustration of MPS molecules grafting on Eucalyptus fibers and interacting with PBS molecules.

Characterization of PBS/r-PET blends and MPS treated Eucalyptus fiber reinforced composites by DSC

The blends of PBS/r-PET were characterized thermal properties by DSC, which Table 3 presents the glass transition temperatures (T_g), the melting temperatures (T_m), and degree of crystallinity (%X_c) of neat PBS, r-PET flake, and PBS/r-PET blends prepared in this study. It was seen that T_g of PBS and r-PET shifted toward each other indicating transesterification occurred between PBS and r-PET molecules during the melt blending. According to Chen and Wu,(18) the ester exchange reaction occurred between PBS and poly(trimethylene terephthalate) during the melt processing, which led to decreasing of interfacial tension that size of dispersed phases was thus reduced sharply.

All the blends exhibited two melting endothermic peaks attributed to PBS matrix and r-PET dispersed phases. Blending PBS with r-PET did not effect on the PBS melting temperatures implying that crystal structure was not altered. This similar behaviour was reported by R.Chen et al. (19) that the crystal type, lamellar thickness and crystal structure of PBS were not affected by compounding with nano-$CaCO_3$ particles. Nevertheless, the degree of crystallinity (X_c) for PBS was reduced when blending with r-PET. According to J. Li et al.,(20) the growth of the PBS crystals was hindered by hollow glass microspheres because they had interfacial interactions with PBS and thus it restricted mobility of PBS chains. Since the X_c of the blends did not increase, the obtained rigidity was mainly reinforced by rigid domains of r-PET in the PBSmatrix.

.

Table 3. Glass transition temperature, melting temperature, and degree of crystallization of neat PBS, r-PET flake, and PBS/r-PET blends.

Materials	T_g [°C]		T_m [°C]		$\Delta H_{m,PBS}$ [J/g]	$\Delta H_{m,PET}$ [J/g]	$\%X_{c,PBS}$	$\%X_{c,PET}$
	PBS	r-PET	PBS	r-PET				
Neat PBS	-32.88	-	113.48	-	64.35	-	58.34	-
r-PET flake	-	80.95	-	247.49	-	37.10	-	26.48
PBS/r-PET 95/5 wt%	-30.57	79.26	112.81	243.78	56.51	2.13	53.93	30.41
PBS/r-PET 90/10 wt%	-30.36	78.61	112.85	243.13	55.54	3.18	55.95	22.70
PBS/r-PET 80/20 wt%	-29.25	78.91	113.59	242.45	50.37	2.70	57.08	9.63

Table 4 Glass transition temperature, melting temperature, and degree of crystallization of PBS/r-PET blends.

Samples	T_g (°C)		T_m (°C)		$\Delta H_{m,PBS}$ [J/g]	$\Delta H_{m,PET}$ [J/g]	$\%X_{c,PBS}$	$\%X_{c,PET}$
	PBS	r-PET	PBS	r-PET				
PBS/r-PET 95/5 wt%	-30.57	79.26	112.81	243.78	56.51	2.13	53.93	30.41
PBS95/r-PET5/Euca3	-30.44	78.96	112.84	243.78	56.00	1.21	55.10	17.81
PBS95/r-PET5/Euca5	-31.32	80.06	113.16	244.08	56.07	1.05	56.33	15.78
PBS95/r-PET5/Euca7	-32.26	80.35	112.88	244.31	55.78	0.97	57.24	14.89
PBS/r-PET 90/10 wt%	-30.36	78.61	112.85	243.13	55.54	3.18	55.95	22.70
PBS90/r-PET10/Euca3	-30.29	84.52	112.92	239.48	50.13	2.86	52.06	21.05
PBS90/r-PET10/Euca5	-29.80	82.38	113.23	239.41	49.74	2.75	38.56	20.66
PBS90/r-PET10/Euca7	-28.00	81.14	113.83	239.85	48.18	2.51	52.19	19.26
PBS/r-PET 80/20 wt%	-29.25	78.91	113.59	242.45	50.37	2.70	57.08	9.63
PBS80/r-PET20/Euca3	-30.37	82.81	113.20	240.31	43.08	5.20	50.33	19.13
PBS80/r-PET20/Euca5	-28.87	82.61	113.49	240.74	43.20	4.53	51.53	17.02
PBS80/r-PET20/Euca7	-27.09	79.09	113.15	240.89	37.21	7.05	45.34	27.05

For MPS treated Eucalyptus fiber reinforced composites, the DSC thermograms showed the similar pattern presenting two glass transition and two melting temperature peaks. Table 4 summarizes the glass transition temperatures (T_g), melting temperatures (T_m), and degree of crystallinity ($\%X_c$) of all composites. It was observed that T_g of PBS matrix was shifted toward higher temperature in the Eucalyptus fiber reinforced composites.This confirmed that the interaction between MPS grafted fibers and PBS matrix, so that higher thermal energy was required for PBS molecules to mobile during the glass transition. For PET, the observed T_g did not show uniform trend because the T_g was influenced by the degree of crystallinity. In contrast to PBS/PET blends, it was found that X_c of PBS increased in low PET content composites, but it was reduced in high PET content composites. This indicated that MPS treated Eucalyptus fibers became nucleating sites for PBS molecules to crystallize. When blending higher PET content, PBS molecules were inhibited by PET molecules to nucleate so that the PBS crystals grew in better compact form showing the melting temperature closed to neat PBS

Conclusions

Eucalyptus fiber reinforced PBS-based composites were successful prepared between biodegradable PBS, post-consumer recycled PET (r-PET) and Eucalyptus fibers. As-received Eucalyptus fibers were alkali treated and then treated with 3 wt% MPS, which FTIR results confirmed grafting of MPS onto Eucalyptus fibers. Blending r-PET into PBS increased Young's modulus, but reduced elongation at break and impact strength of the PBS/r-PETblends. Fiber reinforced composites had higher Young's modulus with respect to fiber loading, however, impact strength of PBS was deteriorated. It was found that composites from PBS/r-PET 95/5 wt% blends showed increasing in impact strength, at which their SEM images revealed that there were fine particles of PET phases dispersed inside PBS matrix and wetting of PBS on silane treated fibers was clearly obtained. Nevertheless, these small dispersed phases of r-PET in higher r-PET content composites became stress concentrators prompting crack propagation, thus composites demonstrated failure toward brittle failure. From DSC results, it was found that T_g of PBS and PET shifted toward each other implying chemical interaction between them via transesterification. Chemical shifts in NMR indicated chemical interaction between PBS and MPS on fibers, which these interactions provided good load transfer between phases that results in rigidity improvement.

Acknowledgements

The authors would like to thank Department of Materials Science and Engineering, Faculty of Engineering and Industrial Technology, Silpakorn University for fully funding this research. We also appreciate SCG Paper Co. Ltd for kindly support alkali treated Eucalyptus fibers.

References

1. Xu J. and Guo B.-H. (2010). Poly(butylene succinate) and its copolymers: Research, development and industrialization, *Bioyechnol J*, **5**: 1149–1163.
2. Nam T. H., Ogihara S., Nakatani H., Kobayashi S. and Song J. I. (2012). Mechanical and thermal properties and water absorption of jute fiber reinforced poly(butylene succinate) biodegradable composites, *Adv Compos Mater*, **21**: 241-258.
3. Feng Y.-H., Zhang D.-W., Qu J.-P., He H.-Z. and Xu B.-P. (2011). Rheological properties of sisal fiber/poly(butylene succinate) composites, *Polym Test*, **30**: 124–130.
4. Frollini E., Bartolucci N., Sisti L. and Celli A. (2013). Poly(butylene succinate) reinforced with different lignocellulosic fibers, *Ind Crop Prod*, **45**: 160–169.
5. Chen R.-y., Zou W., Zhang H.-c., Zhang G.-z., Yang Z.-t., Jin G. and Qu J.-p. (2015). Thermal behavior, dynamic mechanical properties and rheological properties of poly(butylene succinate) composites filled with nanometer calcium carbonate, *Polym Test*, **42**: 160-167.
6. Ali F. B. and Mohan R. (2010). Thermal, mechanical, and rheological properties of biodegradable polybutylene succinate/ carbon nanotubes nanocomposites, *Polym Composite*, **31**: 1309–1314.
7. Hongsriphan N., Popanna A., Arrtith Eksirinimit, Naneraksa P. and Soponsiriwat S. (2014). Mechanical properties of biodegradable poly(butylene succinate) blended with poly (ethylene terephthalate) recycle, ANTEC 2014.
8. Phua Y. J., Lau N. S., Sudesh K., Chow W. S. and Ishak Z.A.M. (2012). Biodegradability studies of poly(butylene succinate)/organo-montmorillonite nanocomposites under controlled compost soil conditions: Effects of clay loading and compatibiliser, *Polym Degrad Stabil*, **97** : 1345-1354.
9. Runt J., Miley D. M., Zhang X., Gallagher K. P., McFeaters K. and Fishburn J. (1992). Crystallization of poly(butylene terephthalate) and its blends with polyarylate, *Macromolecules*, **25**: 1929–1934.
10. Sun S.-N., Cao X.-F., Li H.-Y., Xu F. and Sun R.-C. (2014). Structural characterization of residual hemicelluloses from hydrothermal pretreated Eucalyptus fiber, *Int J Biol Macromol*, **6**: 158–164.

11. Redondo S. U. A., Radovanovic E., Goncalves M. C. and Yoshida I. V. P. (2002). Eucalyptus kraft pulp fibers as an alternative reinforcement of Silicone composites. I. Characterization and chemical modification of Eucalyptus fibers with organosilane coupling agent, *J Appl Polym Sci*, **85**: 2573–2579.

12. Tham W. L., Chow W. S. and Ishak Z. A. M. (2010). The effect of 3-(trimethoxysilyl) propyl methacrylate on the mechanical, thermal, and morphological properties of poly(methylethacrylate)/hydroxyapatite composites, *J Appl Polym Sci*, **118**: 218–228.

13. Arrieta M. P., López J., López D., Kenny J. M. and Peponi L. (2015). Development of flexible materials based on plasticized electrospun PLA–PHB blends: Structural, thermal, mechanical and disintegration properties, *Eur Polym J,* **73**: 433–446.

14. Pawlak A., Morawiec J., Pazzagli F., Pracella M. and Galeski A. (2002). Recycling of Postconsumer Poly(ethylene terephthalate) and High-Density Polyethylene by Compatibilized Blending, *J Appl Polym Sci*, **86**: 1473–1485.

15. Calcagno C. I. W., Mariani C. M., Teixeira S. R. and Mauler R. S. (2008). The role of the MMT on the morphology and mechanical properties of the PP/PET blends, *Compos Sci Technol,* **68**: 2193–2200.

16. Thirunavukarasu K., Purushothaman S., Sridevi J., Aarthy M., Gowthaman M. K., Nakajima-Kambe T. and Kamini N.R. (2016). Degradation of poly(butylene succinate) and poly(butylene succinate-co-butylene adipate) by a lipase from yeast Cryptococcus sp. grown on agro-industrial residues', *Int Biodeter Biodegr*, **110**: 99-107.

17. Kuan C.-F., Ma C.-C. M., Kuan H.-C., Wu H.-L. and Liao Y.-M. (2006). Preparation and characterization of the novel water-crosslinked cellulose reinforced poly(butylenesuccinate) composites, *Compos Sci Technol*, **66**: 2231–2241.

18. Chen J. and Wu D. (2014). Poly(trimethylene terephthalate)/Poly(butylene succinate) blend: Phase behavior and mechanical property control using its transesterification system as the compatibilizer, *Mater Chem Phys*, **148**: 554-561.

19. Chen R., Zou W., Zhang H., Zhang G., Yang Z., Jin G., and Qu J. (2015). Thermal behavior, dynamic mechanical properties and rheological properties of poly(butylene succinate) composites filled with nanometer calcium carbonate, *Polm Test*, **42**: 160-167.

20. Li J., Luo X. and Lin X. (2013). Preparation and characterization of hollow glass microsphere reinforced poly(butylene succinate) composites', *Mater Des*, **46**: 902–909.